DOI: 10.1002/chem.201001564

Assembly of Carbon–SnO_2 Core–Sheath Composite Nanofibers for Superior Lithium Storage

Liwen Ji, Zhan Lin, Bingkun Guo, Andrew J. Medford, and Xiangwu Zhang*[a]

Development of environmentally benign, sustainable, and renewable energy technologies is recognized to be economically and environmentally critical. The most promising energy sources, such as solar power, wind, and ocean waves, are highly variable and will ultimately require coupling to an advanced energy storage technology. Among various alternative energy storage technologies, rechargeable lithium ion batteries (LIBs) with large energy density, high output voltage, and long lifespans may be the most viable system to power increasingly emerging large-scale applications, such as next-generation hybrid/plug-in hybrid electric vehicles and advanced power load leveling for smart grids. The development of improved LIBs is an important step toward the worldwide imperative to replace the slowly, but inevitably vanishing fossil fuel, and, at the same time, avoid negative effects from the current combustion-based energy technologies on global climate change, long-lasting environmental pollution, and human health.[1–6]

Owing to the strong dependence on materials to dictate rechargeable LIB performance, the hunt for nanosized or nanostructured high-performance LIB electrode materials remains the main research objective and also plays a key role in the paradigm shift from the current combustion-based energy technologies to cheap and sustainable energy supply of rechargeable LIBs.[3,7] SnO_2-based materials have displayed extraordinary electrochemical behavior and can theoretically generate much greater specific capacities ($\approx$783 mAh g^{-1}) than state-of-the-art graphite anode, which has a theoretical reversible capacity of about 372 mAh g^{-1}. Unfortunately, pure SnO_2 suffers from a large volume change during lithium alloying and dealloying, which jeopardizes the mechanical integrity of SnO_2-based electrodes; as a result, the materials become pulverized and the batteries using such materials face very rapid capacity fading during charge/discharge cycling.[3,8,9] Recent work has revealed a potential solution to this problem by preparing hierarchically complex structured nanometer-scale SnO_2/carbon composites.[9–13] Here, the carbon matrix can accommodate the mechanical stress induced by the huge volume expansion and shrinkage of high-capacity SnO_2 during lithium insertion/extraction processes, thus preventing deterioration and preserving the integrity of the anodes. One-dimensional SnO_2/C nanocomposites have shown an especially high level of originality and sophistication in recent years[14–17] due to their outstanding features in micromorphology and microstructure, such as distinctive electrical contact to the current collector, facile strain relaxation and excellent material durability, short Li diffusion pathways, ultrahigh transport rate for both Li ions and electrons, and unique electronic conduction.[18–28]

Recently, electrospinning technology has been utilized to fabricate a wide variety of polymer nanofibers as well as carbon nanofibers (CNFs) derived from polymer precursors, such as polyacrylonitrile.[7,21,22,29–32] Electrodeposition is another powerful and fascinating process to synthesize 1D metal oxide nanoscale materials, and it is inexpensive, controllable, and can be carried out at room temperature because of the high energy density accumulated in solution near the electrode surface.[33–35] These two processes have been successfully employed for the preparation of CNFs and transition-metal oxide nanostructured materials, respectively; however, there are few reports on using the combined process to prepare 1D nanocomposites or exploring the potential applications of such composites in rechargeable LIBs.

Herein, we present a novel, effective, simple, and versatile processing strategy for the fabrication of unique carbon–SnO_2 core–sheath composite nanofibers (CSCSCNs) with adjustable sheath thicknesses, involving the electrodeposi-

[a] L. Ji,[+] Z. Lin,[+] B. Guo, A. J. Medford, Prof. X. Zhang
Fiber and Polymer Science Program
Department of Textile Engineering
Chemistry and Science, North Carolina State University
Raleigh, NC 27695-8301 (USA)
Fax: (+1) 919-515-6532
E-mail: xiangwu_zhang@ncsu.edu

[+] These two authors contributed equally to this work.

Supporting information for this article is available on the WWW under http://dx.doi.org/10.1002/chem.201001564.

tion of SnO_2 from a $SnCl_2+H_2SO_4$ solution in the form of thin overlayers that coat CNFs obtained from carbonizing electrospun PAN nanofibers at 600 °C under an argon atmosphere. These materials can then be used as anodes for rechargeable LIBs without adding any polymer binder or additive (Figure 1). These CSCSCN anodes can accommodate large volume changes without pulverization upon Li insertion/extraction processes, show excellent reversible capacity of nearly 800 mAh g^{-1} at the first cycle, and significant capacity retention during the following cycles. In addition, because of their high surface area to volume ratio, CSCSCN anodes also offer fast charge–discharge kinetics even at a high current density of 1000 mA g^{-1}.

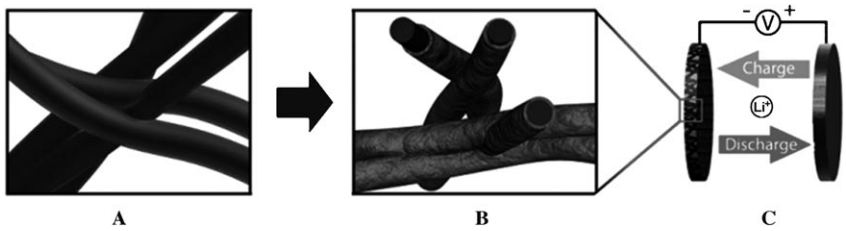

Figure 1. Representation of the preparation of CSCSCNs and their utilization as anodes for rechargeable LIBs. A) CNFs, B) CSCSCNs, and C) Rechargeable LIBs.

Figure 2 A shows an SEM image of electrospun PAN nanofibers with an average diameter at about 300 nm. When thermally treated, the diameters of the fibers decrease (Figure 2 B) because of the weight loss along with the evolution of various gases during the carbonization process. After SnO_2 electrodeposition in an H_2SO_4 environment for 10 h, the diameter of the CNFs increases again. The typical dimensions are about 250 nm in diameter for CSCSCNs, which suggests the formation of a thick layer of SnO_2 coating (Figure 2 C–F).

The high-resolution TEM images in Figure 3 A–B further display a thick layer of electrodeposited SnO_2 on the CNFs. These CSCSCNs have a sheath thickness of about 50 nm, which can be further identified by the cross-sectional TEM analyses shown in Figure 3 C and D. The energy-dispersive X-ray spectroscopy (EDS) analysis in Figure 3 E also confirms the presence of SnO_2 in the electrodeposited CSCSCNs. The wide-angle X-ray diffraction (WAXD) pattern with the clear characteristic peaks of SnO_2 indicate the formation of C/SnO_2

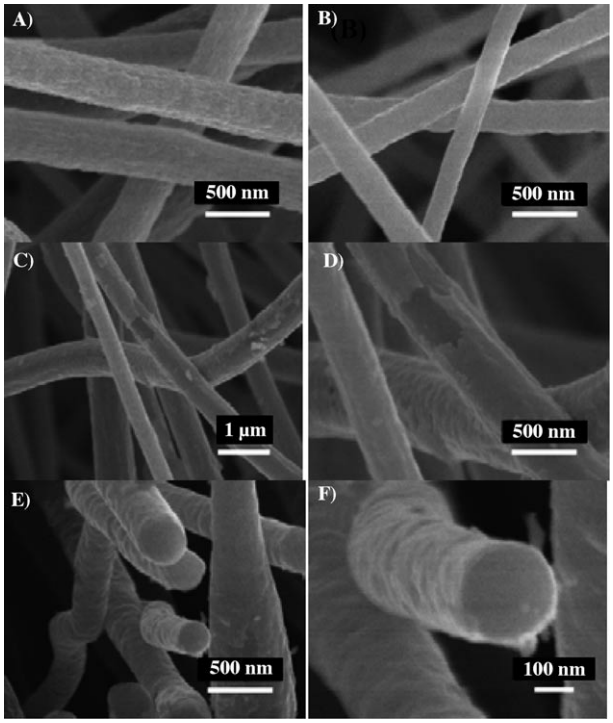

Figure 2. SEM images of pure PAN nanofibers (A), CNFs (B), CSCSCNs (C, D) and the corresponding cross-sectional images of CSCSCNs (E, F). SnO_2 deposition time: 10 h.

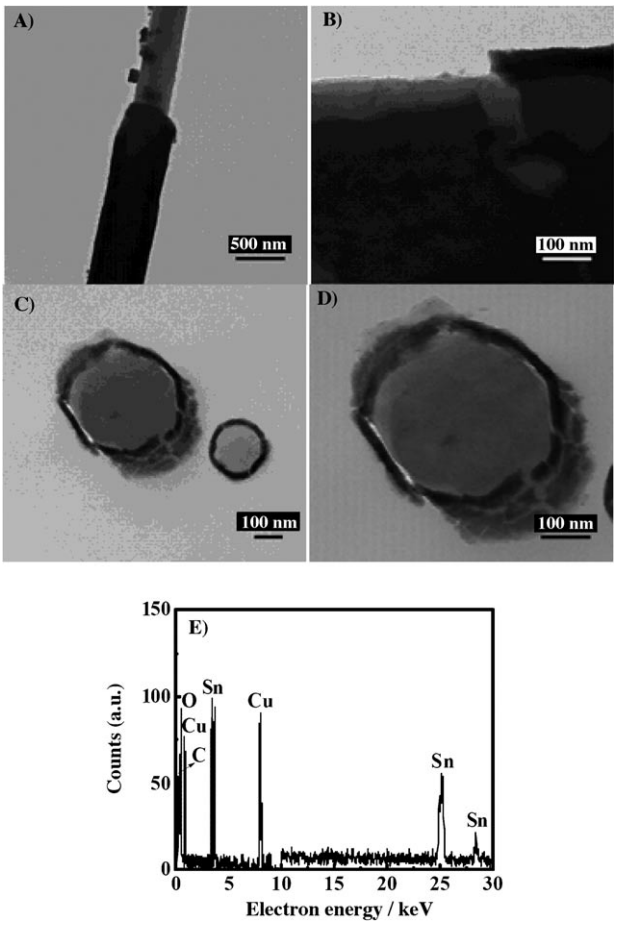

Figure 3. TEM images of CSCSCNs (A, B), cross-sectional TEM images (C, D) and the corresponding EDS spectrum (E). SnO_2 deposition time: 10 h.

nanocomposites (Figure S1 in the Supporting Information). Element analysis shows that these CSCSCNs, prepared with 10 h electrodeposition time, contain about 13.3 % SnO_2.

The electrodeposition of SnO_2 was typically considered to involve the formation of hydroxyl ions on the electrode surface because of the reduction of the acidic group; the further reaction of OH^- ions formed on the electrode surface with tin(II) ions from the bulk solution leads to the formation of nanocrystalline SnO_2.[33–35] In our experiments, CNFs were used as the working electrode and were cycled in 1.0 M H_2SO_4 before electrodeposition to oxidize the surfaces, while breaking bonds and leaving behind negatively charged functional groups, such as carboxyl, carbonyl, and hydroxyl, which can attract tin(II) ions during electrodeposition.[36,37] At the same time, in an acidic environment, SO_4^{2-} ions are electrochemically reduced at the surface of the CNFs, producing a large amount of OH^- in the vicinity of the CNF electrodes. The final reaction of tin(II) ions with OH^- leads to the precipitation of SnO_2 along a continuously propagating reaction front and finally forms a dense and adherent SnO_2 coating on the modified CNF surfaces.[33–35]

To investigate the potential application of the CSCSCNs as anodes in rechargeable LIBs, we explored the electrochemical properties with respect to Li insertion/extraction reactions in coin-type half-cells. Figure 4 A shows the cyclic voltammograms for the initial three cycles at a scan rate of 0.05 mV s^{-1} in the potential window of 3 V to 5 mV. In the first cathodic sweep, one could observe a clear, sharp reduction peaks at about 0.80 V, which is absent in pure CNF-based anodes (Figure S2 in the Supporting Information) and can be ascribed to the transformation of SnO_2 and Li ions to Sn and Li_2O, respectively, as well as the electrolyte decomposition when SnO_2 phases react with Li.[9,10,14,38]

Figure 4 B shows the voltage profile of the prepared CSCSCN anodes during the 1st, 2nd, 20th, 70th, and 100th cycles at 50 mA g^{-1} current density with a cutoff voltage window of 2.8 V to 5 mV. As shown in Figure 4 B, these materials can deliver a large charge capacity of 1136 mAh g^{-1} at the first cycle, followed by a large reversible capacity of about 782 mAh g^{-1} (69 % Coulombic efficiency). The initial irreversible capacity of 354 mAh g^{-1} is attributed to the irreversible reduction of SnO_2 to Sn and other possible irreversible processes.[10,11,16,38] A plateau appears at around 0.8 V, which is not present in pure CNF-based anode (Figure S3 A in the Supporting Information) and can be identified as the reduction of SnO_2 (to metallic Sn and Li_2O), the decomposition of electrolyte, and the formation of solid electrolyte impedance (SEI) film on the produced Sn surface. This plateau disappears after the first cycle, which is in agreement with the CV results in Figure 4 A. This electrochemical behavior is also similar to those of other reported SnO_2/C nanocom-

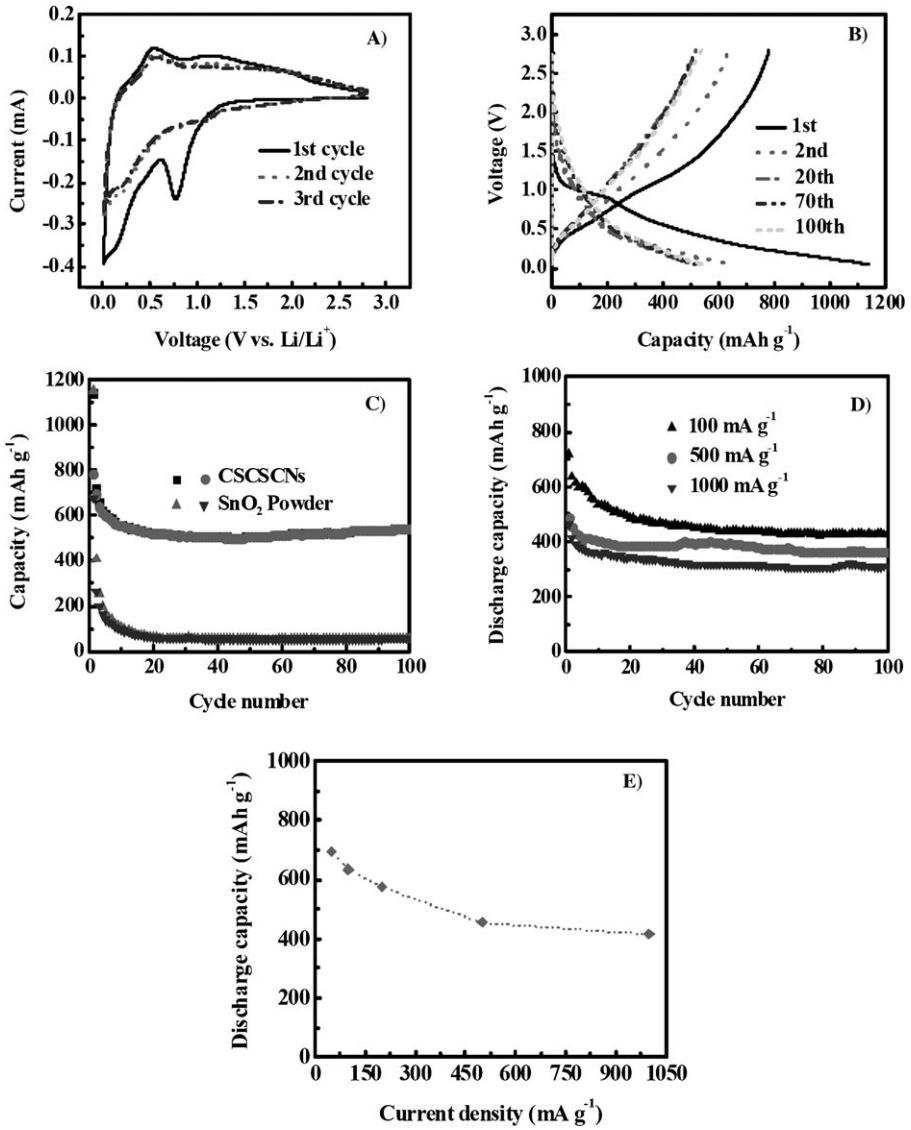

Figure 4. A) Cyclic voltammetry (CV) curves at a scanning rate of 0.05 mV s^{-1}. Charge-discharge curves (B) and cycling performance (C) of CSCSCN anodes at a constant current density of 50 mA g^{-1}. D) Cycling performance of CSCSCN anodes at different current densities. E) Reversible capacity versus current density (rate capability) of CSCSCN anodes. SnO_2 deposition time: 10 h.

posites.[10,39,40] After the formation of Li_xSn, Li ion insertion and extraction reactions proceed reversibly,[9,10,38,40–42] and hence, the irreversible capacity becomes lower.

The cyclability of the CSCSCN anodes was compared with that of pure SnO_2 powder anodes at 50 mA g^{-1} in the voltage window of 5 mV to 2.8 V (Figure 4C). The as-prepared CSCSCN anodes can have a large reversible capacity of about 695 mAh g^{-1} at the second cycle with a 96% coulombic efficiency, and the Coulombic efficiency increases to nearly 100% after the 5th cycle. The reversible capacity at the 100th cycle is about 540 mAh g^{-1}, which corresponds to 69% capacity retention from the first cycle. The average capacity fade rate was hence only 0.31% per cycle in the first 100 cycles. In comparison, the pure SnO_2 powder-based anodes have poor cycling performance. For example, at the first cycle, SnO_2 powder-based anodes can deliver a relatively high initial reversible capacity of about 679 mAh g^{-1}. But severe capacity degradation occurs within the next 20 cycles, leading to a reversible capacity of 62 mAh g^{-1} at the 20th cycle, as shown in Figure 4C. At the 100th cycle, this value decreases to about 55 mAh g^{-1}, indicating rapid capacity degradation with only 8.1% retention from the first cycle. Figure 4C demonstrates that the long-term cycling performance of CSCSCN anodes is drastically enhanced in comparison with that of the bare SnO_2 powders.

These CSCSCNs were also examined with Li ion insertion/extraction at different current densities of 100, 200, 500, and 1000 mA g^{-1}. As shown in Figure 4D, the second-cycle reversible capacities at these current densities are 634, 574, 454, and 415 mAh g^{-1}, respectively. Therefore, when the current density increases from 100 to 1000 mAh g^{-1}, CSCSCN anodes retain 65.5% of the capacity, indicating good rate performance. The further cycling results shown in Figure 4E indicate that the reversible capacities still can be maintained at about 429, 361, and 312 mAh g^{-1}, respectively, after 100 cycles under 100, 500, and 1000 mA g^{-1} current densities, indicating 32.3, 20.5, and 24.8% capacity losses compared with the second cycle capacities at the corresponding current densities. These values, still comparable to the theoretical capacity of graphite, are superior in comparison with those of pure SnO_2 powder-based anodes as shown in Figure S4 in the Supporting Information, and also surpass the results we have observed from pure CNF-based anodes as shown in Figure S3 and other reported results.[29,30] The improvement in rate capability by the CSCSCN anodes is, therefore, significant.

The electrochemical performance of CSCSCN anodes deposited for 20 h was also explored (containing about 16.4% SnO_2). The materials can have a large reversible capacity of about 860 mAh g^{-1} with a 70.2% Coulombic efficiency at the first cycles at 50 mA g^{-1} current density (Figure S5A in the Supporting Information). This reversible capacity retention is about 57.4% after 100 charge/discharge cycles (Figure S5B in the Supporting Information). In addition, these materials also have high reversible capacity and excellent cycle life at high current densities, as shown in Figure S5C and D in the Supporting Information.

Compared with the traditional electrode structure, 1D composite nanofibers could provide more reaction sites on the surface, creating more surface area available for Li ion diffusion, and a shorter Li ion diffusion pathway arising from the nanometer-scale carbon core/SnO_2 sheath structure. The small diameters of CSCSCNs provide enhanced charge transfer and electron conduction along electrodes and decrease the inner resistance of anodes. These are desirable attributes for facilitating Li ion and electron transport that results in a good rate capability. In addition, these CSCSCN anodes can withstand large volume expansion and contraction during Li insertion/extraction processes because of the electronically conducting and mechanically stable CNF cores, which can also function as efficient electron-transport pathways and stable mechanical supports, and keep the structural integrity of the electrodes during cycling. Furthermore, the large surface area and high surface area to volume ratio of core–sheath nanofibers would allow a more efficient Li ion diffusion from both exterior and interior surfaces, resulting in a more symmetric volume transformation and higher Li storage.[13,16,17,38,40]

After Li insertion/extraction, we also explored the morphology and structural changes of cycled CSCSCN anodes. Four samples electrochemically evaluated at different cycle numbers and current rates were disassembled and characterized by using SEM. It was noted that their original nanofibrous morphologies and structures were clearly maintained in all of these samples after cycling (Figure S6 in the Supporting Information).

It should be noted that although the electrochemical performance of our prepared CSCSCN anodes was plagued by some other reported core–sheath nanostructured anodes, such as C–Si[19,20] and C–Sn composites,[21,22] and also did not have an edge over some prepared SnO_2–C core–sheath nanofibrous structures,[14,16] nanospheres,[9,11] or other structure composites, as summarized in Table 1 in the Supporting Information. However, this electrospinning/-deposition combined approach is highly effective, easy to manipulate, non-destructive, low cost, environmentally benign, and it can also avoid the utilization of harsh and destructive chemical/physical processes that involve additional toxic and corrosive chemicals/agents. This approach opens an efficient new avenue for the fabrication of new carbon–metal oxide core–sheath nanocomposite electrodes for rechargeable LIBs and other applications. In addition, through further thermal treatment processes in an Ar/H_2 environment, C–Sn core–sheath nanofibers can be obtained, which may have further improved electrochemical performance when used as anodes for rechargeable LIBs.

In summary, we have creatively prepared CSCSCNs in a controllable fashion through simple and convenient electrospinning and electrodeposition strategies. These as-prepared core–sheath composite nanofibers were tested as binder-free anodes for highly reversible lithium storage, delivering nearly 800 mAh g^{-1} discharge capacity at the first cycle at 50 mA g^{-1} current rate, with 69% capacity retention even after 100 charge/discharge cycles, reflecting significant im-

provement over pure SnO_2 powder-based anodes. In addition, when measured at higher current densities, these nanocomposites also exhibit clearly improved cyclability and rate capability compared with the pure SnO_2 counterparts. These core–sheath structures incorporate simultaneously the unique electrical conductivity of carbon and also the high Li storage ability of SnO_2, and their unique core–sheath structure can prevent the large stresses and volume changes upon Li insertion/extraction processes and help maintain the mechanical stability and structural integrity of the electrodes. These special structures can also have other advantages, such as increased reaction sites for Li, enhanced transport rate for both Li ions and electrons, and improved electrochemical kinetics. As a result, excellent electrochemical performance, such as high Li storage capacity, long charge–discharge cycle life, and increased rate performance, is obtained.

Experimental Section

A solution of 8 wt% PAN in DMF (40 mL) was prepared at 60 °C, with mechanical stirring for at least 24 h. The electrospinning of PAN nanofibers was carried out with a flow rate of 0.5 mL h^{-1}, a needle to collector distance of 15 cm, and an applied voltage of 14 kV. The electrospun PAN nanofibers were first stabilized in air environment at 280 °C for 6 h (heating rate was 5 °C min^{-1}) and then carbonized at 600 °C for 8 h in an argon atmosphere (heating rate was 2 °C min^{-1}) to form CNFs. The resultant CNFs were used as the working electrode in the electrodeposition of SnO_2.

Before electrodeposition, CNFs were oxidized in 1 M H_2SO_4 solution by cyclic voltammetry between −0.7 and 1.2 V at a scan rate of 50 mV s^{-1} for 100 cycles, and then used as the working electrode for the deposition of SnO_2 by applying a potential of −0.2 V (vs. Ag/AgCl/4.0 M KCl) with different deposition durations in a 0.02 M $SnCl_2$ + 0.1 M H_2SO_4 solution. The electrodeposition of SnO_2 onto CNFs was performed on an AQ4 Gamry Reference 600 electrochemical workstation at 25 °C using a three-electrode cell, which consisted of a working electrode (CNFs), a counter electrode (Pt wire), and a reference electrode (Ag/AgCl/4.0 M KCl). Argon was used to bubble the solution for at least 30 min before electrodeposition, and then was used continually to protect the experiment environment. After electrodeposition, the as-prepared CSCSCNs were calcinated at 600 °C for 1 h in Argon and used as the anodes for rechargeable LIBs.

The morphology and diameter of PAN precursor nanofibers, CNFs, and CSCSCNs were evaluated by using SEM (JEOL 6400F Field Emission microscope at 5 kV) and TEM (Hitachi HF-2000 microscope at 200 kV). The structural variations of these prepared nanofibers were also identified by WAXD (Philips X'Pert PRO MRD HR X-ray Diffraction System).

Cyclic voltammetry measurements were performed on AQ4 Gamry Reference 600 electrochemical workstation in the voltage range of 0.01–3 V at a scan rate of 0.05 mV s^{-1}. Electrochemical performance was evaluated by using 2032 coin-type cells (Hohsen). CSCSCNs were attached onto copper foils to be directly used as the working electrode. The pure SnO_2 powder-based working electrodes were prepared by mixing the SnO_2 powders (325 mesh, Sigma), carbon black, and polyvinylidene difluoride at a weight ratio of 80:10:10. The slurry was pasted on pure copper foil and dried in an oven at 70 °C for 12 h, and then in a vacuum oven at 120 °C for 12 h. Lithium ribbon (0.38 mm thick, Aldrich) was used as the counter and reference electrodes. Separion S240 P25 (Degussa AG, 25 μm) was used as the separator. The electrolyte used was 1 M lithium hexafluorophosphate ($LiPF_6$), dissolved in 1/1 (v/v) ethylene carbonate/ethyl methyl carbonate (EMC) (Ferro). Coin cells were assembled in a high-purity argon-filled glovebox. Charge (lithium insertion) and discharge (lithium extraction) were conducted by using an Arbin automatic battery cycler at several different current densities between cutoff potentials of 0.05 and 2.80 V.

Acknowledgements

This study was supported by the Department of Energy (DE-EE0001177), the U.S. National Science Foundation (no. 0833837), and the ERC Program of the National Science Foundation under Award Number EEC-08212121.

Keywords: carbon nanofibers · energy storage · lithium · sustainable chemistry · tin oxide

[1] D. Deng, M. G. Kim, J. Y. Lee, J. Cho, *Energy Environ. Sci.* **2009**, *2*, 818.
[2] Y. S. Hu, R. Demir-Cakan, M. M. Titirici, J. O. Muller, R. Schlogl, M. Antonietti, J. Maier, *Angew. Chem.* **2008**, *120*, 1669; *Angew. Chem. Int. Ed.* **2008**, *47*, 1645.
[3] M. G. Kim, J. Cho, *Adv. Funct. Mater.* **2009**, *19*, 1497.
[4] A. Manthiram, A. V. Murugan, A. Sarkar, T. Muraliganth, *Energy Environ. Sci.* **2008**, *1*, 621.
[5] Y. K. Sun, S. T. Myung, B. C. Park, J. Prakash, I. Belharouak, K. Amine, *Nat. Mater.* **2009**, *8*, 320.
[6] Y. F. Shi, B. K. Guo, S. A. Corr, Q. H. Shi, Y. S. Hu, K. R. Heier, L. Q. Chen, R. Seshadri, G. D. Stucky, *Nano Lett.* **2009**, *9*, 4215.
[7] J. M. Tarascon, N. Recham, M. Armand, J. N. Chotard, P. Barpanda, W. Walker, L. Dupont, *Chem. Mater.* **2010**, *22*, 724.
[8] F. Cheng, Z. Tao, J. Liang, J. Chen, *Chem. Mater.* **2008**, *20*, 667.
[9] X. W. Lou, C. M. Li, L. A. Archer, *Adv. Mater.* **2009**, *21*, 2536.
[10] R. Demir-Cakan, Y. S. Hu, M. Antonietti, J. Maier, M. M. Titirici, *Chem. Mater.* **2008**, *20*, 1227.
[11] X. W. Lou, Y. Wang, C. L. Yuan, J. Y. Lee, L. A. Archer, *Adv. Mater.* **2006**, *18*, 2325.
[12] M. Noh, Y. Kwon, H. Lee, J. Cho, Y. Kim, M. G. Kim, *Chem. Mater.* **2005**, *17*, 1926.
[13] H. X. Zhang, C. Feng, Y. C. Zhai, K. L. Jiang, Q. Q. Li, S. S. Fan, *Adv. Mater.* **2009**, *21*, 2299.
[14] M. S. Park, Y. M. Kang, S. X. Dou, H. K. Liu, *J. Phys. Chem .C* **2008**, *112*, 11286.
[15] J. F. Ye, H. J. Zhang, R. Yang, X. G. Li, L. M. Qi, *Small* **2010**, *6*, 296.
[16] Y. Wang, H. C. Zeng, J. Y. Lee, *Adv. Mater.* **2006**, *18*, 645.
[17] F. F. Cao, Y. G. Guo, S. F. Zheng, X. L. Wu, L. Y. Jiang, R. R. Bi, L. J. Wan, J. Maier, *Chem. Mater.* **2010**, *22*, 1908.
[18] C. K. Chan, H. L. Peng, G. Liu, K. McIlwrath, X. F. Zhang, R. A. Huggins, Y. Cui, *Nat. Nanotechnol.* **2008**, *3*, 31.
[19] L. F. Cui, Y. Yang, C. M. Hsu, Y. Cui, *Nano Lett.* **2009**, *9*, 3370.
[20] H. Kim, J. Cho, *Nano Lett.* **2008**, *8*, 3688.
[21] Y. Yu, L. Gu, C. L. Wang, A. Dhanabalan, P. A. van Aken, J. Maier, *Angew. Chem.* **2009**, *121*, 6607; *Angew. Chem. Int. Ed.* **2009**, *48*, 6485.
[22] Y. Yu, L. Gu, C. B. Zhu, P. A. van Aken, J. Maier, *J. Am. Chem. Soc.* **2009**, *131*, 15984.
[23] C. K. Chan, X. F. Zhang, Y. Cui, *Nano Lett.* **2008**, *8*, 307.
[24] L. F. Cui, R. Ruffo, C. K. Chan, H. L. Peng, Y. Cui, *Nano Lett.* **2009**, *9*, 491.
[25] H. Lee, J. Cho, *Nano Lett.* **2007**, *7*, 2638.
[26] Y. G. Li, B. Tan, Y. Y. Wu, *Nano Lett.* **2008**, *8*, 265.
[27] M. H. Park, M. G. Kim, J. Joo, K. Kim, J. Kim, S. Ahn, Y. Cui, J. Cho, *Nano Lett.* **2009**, *9*, 3844.
[28] J. Zhang, Y. S. Hu, J. P. Tessonnier, G. Weinberg, J. Maier, R. Schlogl, D. S. Su, *Adv. Mater.* **2008**, *20*, 1450.

[29] L. W. Ji, Z. Lin, A. J. Medford, X. W. Zhang, *Chem. Eur. J.* **2009**, *15*, 10718.
[30] L. W. Ji, Z. Lin, A. J. Medford, X. W. Zhang, *Carbon* **2009**, *47*, 3346.
[31] D. Li, Y. N. Xia, *Adv. Mater.* **2004**, *16*, 1151.
[32] J. T. McCann, B. K. Lim, R. Ostermann, M. Rycenga, M. Marquez, Y. N. Xia, *Nano Lett.* **2007**, *7*, 2470.
[33] S. T. Chang, I. C. Leu, M. H. Hon, *Electrochem. Solid-State Lett.* **2002**, *5*, C71.
[34] M. Lai, J. H. Lim, S. Mubeen, Y. Rheem, A. Mulchandani, M. A. Deshusses, N. V. Myung, *Nanotechnology* **2009**, *20*, 185602.
[35] M. Lai, J. A. G. Martinez, M. Gratzel, D. J. Riley, *J. Mater. Chem.* **2006**, *16*, 2843.
[36] S. L. Knupp, W. Z. Li, O. Paschos, T. M. Murray, J. Snyder, P. Haldar, *Carbon* **2008**, *46*, 1276.
[37] Z. Lin, L. Ji, M. D. Woodroof, Y. Yao, W. Krause, X. Zhang, *J. Phys. Chem. C* **2010**, *114*, 3791.
[38] M. S. Park, G. X. Wang, Y. M. Kang, D. Wexler, S. X. Dou, H. K. Liu, *Angew. Chem.* **2007**, *119*, 764; *Angew. Chem. Int. Ed.* **2007**, *46*, 750.
[39] C. Kim, M. Noh, M. Choi, J. Cho, B. Park, *Chem. Mater.* **2005**, *17*, 3297–3301.
[40] Y. Wang, J. Y. Lee, H. C. Zeng, *Chem. Mater.* **2005**, *17*, 3899–3903.
[41] J. Liu, W. Li, A. Manthiram, *Chem. Commun.* **2010**, *46*, 1437.
[42] X. W. Lou, D. Deng, J. Y. Lee, L. A. Archer, *Chem. Mater.* **2008**, *20*, 6562.

Received: June 3, 2010
Published online: September 8, 2010

